UDC 54.057; 547.022; 615.212; 615.398
DOI: 10.15587/2519-4852.2025.323594

SYNTHESIS, ANTICANCER PROPERTIES EVALUATION AND IN SILICO STUDIES OF 2-CHLORO- AND 2,2-DICHLOROACETAMIDES BEARING THIAZOLE SCAFFOLDS

Liubomyr Havryshchuk, Volodymyr Horishny, Iryna Ivasechko, Yuliia Kozak, Dmytro Melnyk, Dmytro Khylyuk, Myroslava Kusiy, Victoria Serhiyenko, Nataliya Finiuk, Rostyslav Stoika, Serhii Holota, Roman Lesyk

The aim. *The study aimed to synthesize and evaluate the anticancer activity of a series of 2-chloro- and 2,2-dichloroacetamides bearing thiazole scaffolds. Particular attention was paid to their cytotoxic effects, chemical properties, and action mechanisms, with a focus on glutathione S-transferase (GST) inhibition as a potential pathway for anticancer activity.*

Materials and methods. *The compounds were synthesized using acylation reactions and characterized via ^{1}H and ^{13}C NMR spectroscopy as well as LC-MS. Their cytotoxicity was assessed using the MTT assay across cancer and pseudo-normal cell lines. Quantum-chemical calculations were performed using DFT, while molecular docking studies analyzed interactions with GST to explore their interaction.*

Results. *Among the synthesized derivatives, 2-chloroacetamides exhibited significant cytotoxic activity against human acute T cell leukemia (Jurkat) and triple-negative breast cancer (MDA-MB-231) cell lines, as well as Ba/F3 cells with calreticulin mutations. In contrast, 2,2-dichloroacetamides showed negligible activity across all tested cell lines. Quantum-chemical analysis indicated that structural and electronic differences between these two compound classes likely influence their bioactivity. Molecular docking studies revealed higher binding affinities of glutathione-2-chloroacetamide conjugates to GST, compared to the reference glutathione-etacrynic acid complex, suggesting GST inhibition as a potential mechanism underlying their anticancer effects.*

Conclusions. *The synthesized 2-chloroacetamides demonstrate promising potential as anticancer agents, likely due to their ability to form inhibitory conjugates with glutathione, thereby affecting GST activity. These findings underline the importance of further studies to optimize these compounds for therapeutic use*

Keywords: *chloroacetamides, dichloroacetamides, aminothiazoles, anticancer activity, quantum-chemical calculations, molecular docking, glutathione, GST inhibition*

How to cite:
Havryshchuk, L., Horishny, V., Ivasechko, I., Kozak, Y., Melnyk, D., Khylyuk, D., Kusiy, M., Serhiyenko, V., Finiuk, N., Stoika, R., Holota, S., Lesyk, R. (2025). Synthesis, anticancer properties evaluation and in silico studies of 2-chloro- and 2,2-dichloroacetamides bearing thiazole scaffolds. ScienceRise: Pharmaceutical Science, 1 (53), 71–82. http://doi.org/10.15587/2519-4852.2025.323594

1. Introduction

Nowadays, the structure diversity of potential anticancer drugs and agents has gained significant progress and achievements; however, small molecules still represent a majority of studied/approved candidates that target different pathways of carcinogenesis [1–5]. In this field of anticancer drug design chloro- (CAAs) and dichloroacetamides (DCAAs) have been the objects of detailed research during the last decades as effective cytotoxic agents [6–10], FGFR- [11], alcohol/aldehyde dehydrogenases (ADH/ALDH) [12], KRAS covalent [13, 14], PARP- [15], pyruvate dehydrogenase kinases (PDKs) inhibitors [16–21], and multi-target agents [22, 23]. This area of chemical space covers simple chemotypes of molecules that are easily accessible with wide variation and structure complexity in amide moieties, making it attractive for the diversity-oriented design [24–26]. While the ability to affect a wide range of molecular targets makes them interesting for pharmacologists. It is worth noting that today, CAAs are widely known and popular as covalent inhibitors [27], and synthetic chemists more often successfully apply these molecules as effective covalent warheads, which was demonstrated in developing KRAS – inhibitors [13, 14]. The anticancer properties of dichloroacetic acid (DCA) were initially reported in the early 2000s and later proved that DCA significantly impacts the growth and survival of tumor cells [28, 29]. Among other established DCA mechanisms of action was an increase in reactive oxygen species. Later, the synthesis of corresponding DCAAs was proposed as a possible structure optimization approach for DCA anticancer and ADMET properties (Fig. 1) [21]. It should be noted that the number of reports in this field is growing yearly, indicating the actuality and need for a deeper study of the anticancer activity of CAAs and DCAAs and the development of these molecules as potential anticancer agents.

Aminothiazole-bearing scaffolds are considered privileged heterocycles in the anticancer drug de-

sign [30, 31]. Incorporation of these fragments into the structure of the basic molecules was applied by medicinal chemists in the design of potential inhibitors to various druggable anticancer molecular targets such as tubulin, histone acetylase/histone deacetylase (HAT/HDAC), different kinases, epidermal growth factor receptor and other [30, 31]. From the perspective of synthetic chemistry, the presence of free amino groups in the molecules of aminothiazole-bearing scaffolds makes them convenient building blocks for the application in the different hybridization (molecular/scaffold/pharmacophore) methodologies.

Considering all the above, in the present paper, the synthesis of a series of structure-related 2-chloro- and 2,2-dichloroacetamides bearing thiazole scaffolds, studies, and comparison of their anticancer and cytotoxicity properties in vitro are reported. Significant attention in the study was devoted to performing quantum chemical calculations and docking simulations to detail the obtained results and predict potential mechanisms for the synthesized compounds.

2. Planning (methodology) of research

Building upon the promising background, this research is planned with a systematic, quality-driven approach. The present paper aims to synthesize a series of 2-chloro- and 2,2-dichloroacetamides bearing thiazole scaffolds and to compare their anticancer and cytotoxicity properties *in vitro*.

The methodology encompasses synthetic procedures, comprehensive physical-chemical characterization (NMR, LC-MS, and elemental analysis), and *in vitro* biological evaluation using MTT assays on various cancer and pseudo-normal cell lines. Additionally, *in silico* techniques, including quantum chemical calculations and molecular docking simulations targeting GST, are employed to elucidate the electronic characteristics and potential action mechanisms. This integrated approach is expected to provide critical insights into the differential reactivity of CAAs versus DCAAs, thereby laying the groundwork for the rational design of more effective targeted anticancer agents. Fig. 1 illustrates the overall research strategy and design.

3. Materials and methods

3. 1. Chemistry

General.

Melting points were measured in open capillary tubes on a BÜCHI B-545 melting point apparatus (BÜCHI Labortechnik AG, Flawil, Switzerland) and were uncorrected. The elemental analyses (C, H, N) were performed using the Perkin-Elmer 2400 CHN analyzer (PerkinElmer, Waltham, MA, USA) and were within ±0.4 % of the theoretical values. The 500 MHz-1H and 126 MHz-13C spectra were recorded on Bruker AVANCE-500 spectrometer (Bruker, Bremen, Germany). All spectra were recorded at room temperature except where indicated otherwise and were referenced internally to solvent reference frequencies. Chemical shifts (δ) are quoted in ppm and coupling constants (*J*) are reported in Hz. LC–MS spectra were obtained on a Finnigan MAT INCOS-50 (Thermo Finnigan LLC, San Jose, CA, USA). Solvents and reagents that are commercially available were used without further purification. Commercially available chloroacetyl chloride (CAS 79-04-9), dichloroacetyl chloride (CAS 79-36-7), 2-amino-2-thiazoline (CAS 1779-81-3), 2-aminothiazole (96-50-4), 2-amino-4-phenylthiazole (CAS 2010-06-2), 2-amino-4-(4-chlorophenyl)thiazole (CAS 2103-99-3), ethyl 2-aminothiazole-4-acetate (CAS 53266-94-7), 2-aminobenzothiazole (CAS 136-95-8), 4,6-dimethyl-benzothiazol-2-ylamine (CAS 64036-71-1), and triethylamine (CAS 121-44-8) were used for the synthesis of the target compounds 2a,b; 3a-h; 4a-d in present research. Synthesis of 2-chloro-N-(thiazol-2-yl)acetamide 3a was early reported in [32], and the physic-chemical properties of the 3a correspond to the data reported in [33].

General procedure for the synthesis of chloroacetamides and dichloroacetamides 2a,b; 3a-h; 4a-d.

A solution of chloroacetyl chloride or dichloroacetyl chloride (3 mmol) in 5 ml of dioxane dropwise was added to the mixture of an appropriate amine (3 mmol) and triethylamine (3 mmol) in 5 ml of dioxane. The obtained mixture was stirred for 15 minutes at r. t. and then was heated to 70–80 °C for 30 minutes. After cooling, the mixture was poured into cold water (50 ml). The obtained powders were filtered off, washed with water, and recrystallized from ethanol.

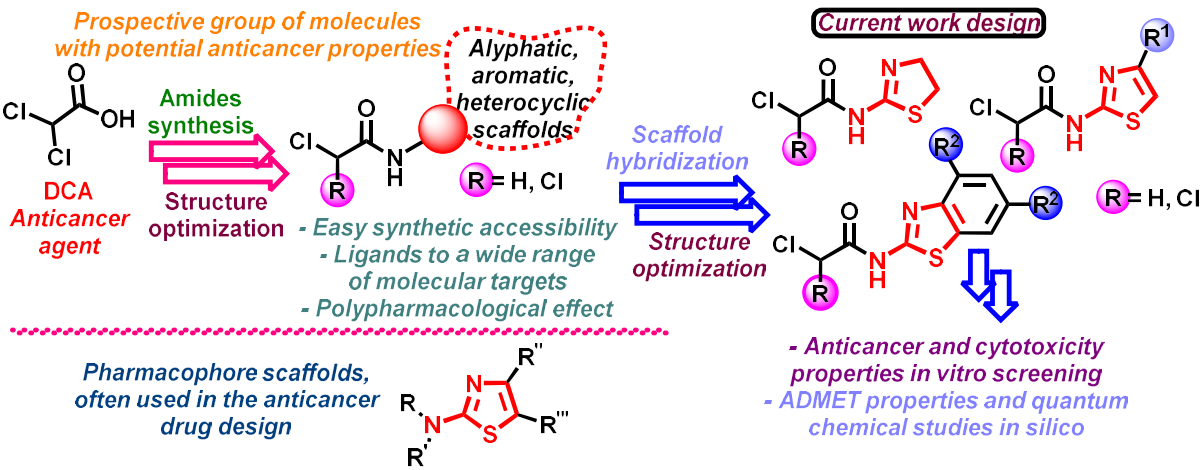

Fig. 1. Background and design of the current studies

2-Chloro-N-(4,5-dihydrothiazol-2-yl)acetamide (2a).

White powder, yield 58 %, mp 131–133 °C (*i*-PrOH). ^{1}H NMR (500 MHz, DMSO-d_6, δ): 9.86 (s, 1H, NH), 4.22 (*s*, 2H, CH_2), 3.63 (*t*, *J*=8.0 Hz, 2H, CH_2), 3.23 (*t*, *J*=8.0 Hz, 2H, CH_2). ^{13}C NMR (126 MHz, DMSO-d_6, δ): 173.7 (C=O), 171.4, 46.2 (CH_2), 45.7 (CH_2), 29.8 (CH_2). LCMS (ESI+) m/z 179.0/181.0 (100.0 %, $[M+H]^+$). Anal. calc. for $C_5H_7ClN_2OS$: C, 33.62 %; H, 3.95 %; N, 15.68 %. Found: C, 33.80 %; H, 4.10 %; N, 15.80 %.

2,2-Dichloro-N-(4,5-dihydrothiazol-2-yl)acetamide (2b).

White powder, yield 64 %, mp 150–152 °C (*i*-PrOH). ^{1}H NMR (500 MHz, DMSO-d_6, δ): 9.91 (*s*, 1H, NH), 6.44 (*s*, 1H, CH), 3.65 – 3.59 (*m*, 2H, CH_2), 3.29 (*td*, *J*=7.9, 4.0 Hz, 2H, CH_2). ^{13}C NMR (126 MHz, DMSO-d_6, δ): 177.5 (C=O), 172.7 (C-2), 70.3 (CH), 44.1(CH_2), 29.42 (CH_2). LCMS (ESI+) m/z 213.0/215.0 (100.0 %, $[M+H]^+$). Anal. calc. for $C_5H_6Cl_2N_2OS$: C, 28.18 %; H, 2.84 %; N, 13.15 %. Found: C, 28.30 %; H, 3.10 %; N, 13.30 %.

2,2-Dichloro-N-(thiazol-2-yl)acetamide (3b).

White powder, yield 73 %, mp 180–182 °C (*i*-PrOH). ^{1}H NMR (500 MHz, DMSO-d_6, δ): 13.01 (*s*, 1H, NH), 7.55 (*d*, *J*=3.7 Hz, 1H, thiazole), 7.33 (*d*, *J*=3.7 Hz, 1H, thiazole), 6.64 (*s*, 1H, CH). ^{13}C NMR (126 MHz, DMSO-d_6, δ): 166.22 (C=O), 160.64 (C-2), 137.61 (C-4), 114.64 (C-5), 66.5 (CH). LCMS (ESI+) m/z 211.0/213.0 (100.0 %, $[M+H]^+$). Anal. calc. for $C_5H_4Cl_2N_2OS$: C, 28.45 %; H, 1.91 %; N, 13.27 %. Found: C, 28.60 %; H, 2.10 %; N, 13.50 %.

2-Chloro-N-(4-phenylthiazol-2-yl)acetamide (3c).

White powder, yield 81 %, mp 147–149 °C (*i*-PrOH). ^{1}H NMR (500 MHz, DMSO-d_6, δ): 12.63 (*s*, 1H, NH), 7.89 (*d*, *J*=7.6 Hz, 2H, arom.), 7.67 (*s*, 1H, thiazole), 7.42 (*t*, *J*=7.5 Hz, 2H, arom.), 7.32 (*t*, *J*=7.6 Hz, 1H, arom.), 4.41 (*s*, 2H, CH_2). ^{13}C NMR (126 MHz, DMSO-d_6, δ): 165.1 (C=O), 164.9, 157.4, 149.0, 134.1, 128.7, 127.8, 125.6, 108.5, 42.3 (CH_2). LCMS (ESI+) m/z 253.0/255.0 (100.0 %, $[M+H]^+$). Anal. calc. for $C_{11}H_9ClN_2OS$: C, 52.28 %; H, 3.59 %; N, 11.09 %. Found: C, 52.40 %; H, 3.80 %; N, 11.20 %.

2,2-Dichloro-N-(4-phenylthiazol-2-yl)acetamide (3d).

White powder, yield 79 %, mp 111–113 °C (EtOH-H_2O 2:1). ^{1}H NMR (500 MHz, DMSO-d_6, δ): 13.08 (*s*, 1H, NH), 7.90 (*d*, *J*=7.6 Hz, 2H, arom.), 7.77 (*s*, 1H, thiazole), 7.43 (*t*, *J*=7.5 Hz, 2H, arom.), 7.34 (*t*, *J*=7.3 Hz, 1H, arom.), 6.68 (*s*, 1H, CH). ^{13}C NMR (126 MHz, DMSO-d_6, δ): 162.1 (C=O), 156.8, 149.5, 133.8, 128.7, 28.0, 125.7, 109.5, 65.8 (CH). LCMS (ESI+) m/z 287.0/289.0 (100.0 %, $[M+H]^+$). Anal. calc. for $C_{11}H_8Cl_2N_2OS$: C, 46.01 %; H, 2.81 %; N, 9.76 %. Found: C, 46.20 %; H, 3.00 %; N, 9.90 %.

2-Chloro-N-(4-(4-chlorophenyl)thiazol-2-yl)acetamide (3e).

White powder, yield 78 %, mp 168–170 °C (*i*-PrOH). ^{1}H NMR (500 MHz, DMSO-d_6, δ): 12.65 (s, 1H, NH), 7.89 (*d*, *J*=7.7 Hz, 2H, arom.), 7.73 (*s*, 1H, thiazole), 7.47 (*d*, *J*=7.7 Hz, 2H, arom.), 4.41 (*s*, 1H, CH_2). ^{13}C NMR (126 MHz, DMSO-d_6, δ): 165.2 (C=O), 157.5, 147.7, 132.9, 132.3, 128.7, 127.3, 109.2, 42.2 (CH_2). LCMS (ESI+) m/z 287.0/289.0 (100.0 %, $[M+H]^+$). Anal. calc. for $C_{11}H_8Cl_2N_2OS$: C, 46.01 %; H, 2.81 %; N, 9.76 %. Found: C, 46.10 %; H, 3.10 %; N, 10.00 %.

2,2-Dichloro-N-(4-(4-chlorophenyl)thiazol-2-yl)acetamide (3f).

White powder, yield 75 %, mp 128–122 °C (*i*-PrOH). ^{1}H NMR (500 MHz, DMSO-d_6, δ): 13.09 (s, 1H, NH), 7.92 (*d*, *J*=8.0 Hz, 2H, arom.), 7.83 (*s*, 1H, thiazole), 7.50 (*d*, *J*=8.0 Hz, 2H, arom.), 6.69 (*s*, 1H, CH). ^{13}C NMR (126 MHz, DMSO-d_6, δ): 162.1 (C=O), 157.0, 148.2, 132.7, 132.5, 128.8, 127.4, 110.2, 65.8 (CH). LCMS (ESI+) m/z 322.0/324.0 (100.0 %, $[M+H]^+$). Anal. calc. for $C_{11}H_7Cl_3N_2OS$: C, 41.08 %; H, 2.19 %; N, 8.71 %. Found: C, 41.20 %; H, 2.40 %; N, 8.90 %.

Ethyl 2-(2-(2-chloroacetamido)thiazol-4-yl)acetate (3g).

White powder, yield 72 %, mp 145–147 °C (EtOH). ^{1}H NMR (500 MHz, DMSO-d_6, δ): 12.54 (*s*, 1H, NH), 7.05 (*s*, 1H, thiazole), 4.35 (*s*, 2H, CH_2), 4.07 (*q*, *J*=7.1 Hz, 2H, CH_2), 3.69 (*s*, 2H, CH_2), 1.18 (*t*, *J*=7.1 Hz, 3H, CH_3). ^{13}C NMR (126 MHz, DMSO-d_6, δ): 169.9 (C=O), 164.8 (C=O), 157.0, 143.9, 110.9, 60.3 (CH_2), 42.2 (CH_2), 36.5 (CH_2), 14.0 (CH_3). LCMS (ESI+) m/z 263.0/265.0 (100.0 %, $[M+H]^+$). Anal. calc. for $C_9H_{11}ClN_2O_3S$: C, 41.15 %; H, 4.22 %; N, 10.66 %. Found: C, 41.40 %; H, 4.40 %; N, 10.80 %.

Ethyl 2-(2-(2,2-dichloroacetamido)thiazol-4-yl)acetate (3h).

White powder, yield 75 %, mp 89–91 °C (EtOH-H_2O 1:1). ^{1}H NMR (500 MHz, DMSO-d_6, δ): 13.01 (*s*, 1H, NH), 7.14 (*s*, 1H, thiazole), 6.62 (*s*, 1H, CH), 4.08 (*s*, 2H, CH_2), 3.73 (*s*, 2H, CH_2), 1.18 (*s*, 3H, CH_3). ^{13}C NMR (126 MHz, DMSO-d_6, δ): 169.7 (C=O), 161.9 (C=O), 156.5, 144.3, 111.9, 66.0 (CH), 60.3 (CH_2), 36.3 (CH_2), 14.05 (CH_3). LCMS (ESI+) m/z 297.0/299.0 (100.0 %, $[M+H]^+$). Anal. calc. for $C_9H_{10}Cl_2N_2O_3S$: C, 36.38 %; H, 3.39 %; N, 9.43 %. Found: C, 36.50 %; H, 3.50 %; N, 9.70 %.

N-(Benzo[d]thiazol-2-yl)-2-chloroacetamide (4a).

White powder, yield 79 %, mp 163–165 °C (*i*-PrOH). ^{1}H NMR (500 MHz, DMSO-d_6, δ): 12.70 (s, 1H, NH), 7.99 (*d*, *J*=7.9 Hz, 1H, arom.), 7.76 (*d*, *J*=8.1 Hz, 1H, arom.), 7.44 (*t*, *J*=7.7 Hz, 1H, arom.), 7.31 (*t*, *J*=7.6 Hz, 1H, arom.), 4.46 (*s*, 2H, CH_2). ^{13}C NMR (126 MHz, DMSO-d_6, δ): 165.8 (C=O), 157.5, 148.4, 131.4, 126.2, 123.7, 121.7, 120.6, 42.5 (CH_2). LCMS (ESI+) m/z 227.0/229.0 (100.0 %, $[M+H]^+$). Anal. calc. for $C_9H_7ClN_2OS$: C, 47.69 %; H, 3.11 %; N, 12.36 %. Found: 47.90 %; H, 3.30 %; N, 12.50 %.

N-(Benzo[d]thiazol-2-yl)-2,2-dichloroacetamide (4b).

White powder, yield 80 %, mp 188–190 °C (*i*-PrOH). $_1$H NMR (500 MHz, DMSO-d_6, δ): 13.28 (s, 1H, NH), 8.01 (*d*, *J*=7.9 Hz, 1H, arom.), 7.74 (*d*, *J*=8.1 Hz, 1H, arom.), 7.47 (*t*, *J*=7.7 Hz, 1H, arom.), 7.35 (*t*, *J*=7.6 Hz, 1H, arom.), 6.71 (*s*, 1H, CH).^{13}C NMR (126 MHz, DMSO-d_6, δ): 163.2 (C=O), 157.0, 147.9, 131.0, 126.6, 124.2, 122.2, 121.0, 64.6 (CH). LCMS (ESI+) m/z 261/263 (100.0 %, $[M+H]^+$). Anal. calc. for $C_9H_6Cl_2N_2OS$: C, 41.40 %; H, 2.32 %; N, 10.73 %. Found: C, 41.60 %; H, 2.50 %; N, 10.90 %.

2-Chloro-N-(4,6-dimethylbenzo[d]thiazol-2-yl)acetamide (4d).

White powder, yield 77 %, mp 196–198 °C (*i*-PrOH). ^{1}H NMR (500 MHz, DMSO-d_6, δ): 12.71 (*s*, 1H, NH), 7.56 (*s*, 1H, arom.), 7.06 (*s*, 1H, arom.), 4.42 (*s*, 2H, CH_2), 2.51 (*s*, 3H, CH_3), 2.49 (*s*, 3H, CH_3). ^{13}C NMR (126 MHz, DMSO-d_6, δ): 165.5 (C=O), 155.6, 145.5, 133.1,

131.2, 129.5, 128.1, 118.7, 42.3 (CH_2), 20.9 (CH_3), 17.7 (CH_3). LCMS (ESI+) m/z 255/257 (100.0 %, $[M+H]^+$). Anal. calc. for $C_{11}H_{11}ClN_2OS$: C, 51.87 %; H, 4.35 %; N, 11.00 %. Found: C, 52.10 %; H, 4.50 %; N, 11.20 %.

2,2-Dichloro-N-(4,6-dimethylbenzo[d]thiazol-2-yl) acetamide (4e).

White powder, yield 80 %, mp 195–197 °C (*i*-PrOH). ^{1}H NMR (500 MHz, DMSO-d_6, δ): 13.18 (*s*, 1H, NH), 7.59 (*s*, 1H, arom.), 7.09 (*s*, 1H, arom.), 6.67 (*s*, 1H, CH), 2.51 (*s*, 3H, CH_3), 2.49 (*s*, 3H, CH_3). ^{13}C NMR (126 MHz, DMSO-d_6, δ): 162.3 (C=O), 155.1, 145.8, 133.6, 131.3, 129.5, 128.4, 118.9, 65.9 (CH), 20.9 (CH_3), 17.7 (CH_3). LCMS (ESI+) m/z 289/291 (100.0 %, $[M+H]^+$). Anal. calc. for $C_{11}H_{10}Cl_2N_2OS$: C, 45.69 %; H, 3.49 %; N, 9.69 %. Found: C, 45.90 %; H, 3.70 %; N, 9.90 %.

3. 2. Assessment of compounds cytotoxicity via MTT assay

The pseudo-normal cell lines BALB-3T3 (mouse embryo fibroblasts) and HaCaT (human epidermal keratinocytes), as well as the cancer cell lines MDA-MB-231 (human triple-negative breast cancer), K562 (human chronic myelogenous leukemia), HT-29 (human colon cancer), and Jurkat (human acute T cell leukemia), were kindly provided by the Collection at the Institute of Molecular Biology and Genetics, National Academy of Sciences of Ukraine (Kyiv, Ukraine). HCT-116 colon cancer cells were donated by the Collection of the Institute for Cancer Research at Vienna Medical University (Vienna, Austria). Ba/F3 cell lines, models for myeloproliferative neoplasms, kindly provided for research by Prof. Robert Kralovics (Vienna Medical University). The cells were maintained in Dulbecco's Modified Eagle Medium (DMEM, Biowest, France) or RPMI-1640 medium (Biowest, France), containing 10 % of fetal bovine serum (FBS, Biowest, France), according to the recommendations of the American Type Culture Collection (ATCC), under the incubation conditions of 5 % CO_2 and 90–95 % humidity at 37 °C.

The viability of cell lines after incubation with the compounds was assessed using 3-[4,5-dimethylthiazol-2-yl]-2,5-diphenyl tetrazolium bromide (MTT reagent) (Sigma-Aldrich, USA) [34]. 6000 Adherent cells or 15,000 suspension cells per well were seeded in 96-well plates in 100 µL of DMEM or RPMI-1640 (Sigma-Aldrich, USA) according to the recommendations of the ATCC and incubated for 24–72 hours at 37 °C in a CO_2 incubator with different concentrations of the studied compounds (3 concentrations (5, 10, and 50 µM) each in 3 replicates). After the incubation period, the test medium was discarded, the MTT reagent was added to the cells according to the manufacturer's recommendations (final concentration 5mg/mL) and incubated for an additional 4 hours. The formazan crystals were dissolved using DMSO, and the absorbance was measured using an Absorbance Reader BioTek ELx800 (BioTek Instruments, Inc., Winooski, VT, USA) at a wavelength of 490 nm. The IC50 values were calculated using GraphPad Prism 8 software (San Diego, California, USA).

3. 3. Quantum – chemical calculations

The structure of the synthesized compounds and intermediate states was optimized using the Gaussian 09 program [35], results were visualized using GaussView 5.0.8 [36]. In all studied structures, the geometry was optimized using density functional theory (DFT) in the B3LYP approach with a standard set of basic functions 6-311++G(d,p).

3. 4. Molecular docking

Potential glutathione-chloroacetamide (GSH-CA) conjugates were constructed by modifying the 3D structure of glutathione with the alkyl groups from the synthesized compounds. The protonation states of the structures were adjusted to reflect physiological pH (7.4). These conjugates were subsequently minimized using a molecular mechanics-based optimization approach. The minimization was performed with the MMFF94 [37, 38] force field in Avogadro software, using a maximum of 10,000 steps [38].

The crystal structure of glutathione S-transferase (GST) (PDB ID: 1lGS) [39] was retrieved from the Protein Data Bank (PDB) for docking studies. For docking simulations, we employed the FlexX algorithm [40] implemented in LeadIT 2.3.2 due to its capability to accurately predict the binding positions of the glutathione-ethacrynic acid complex. The algorithm demonstrated sufficient accuracy, with root mean square deviation (RMSD) values of less than 2 Å (observed RMSD: 1.8402 Å) (Fig. 2) [41].

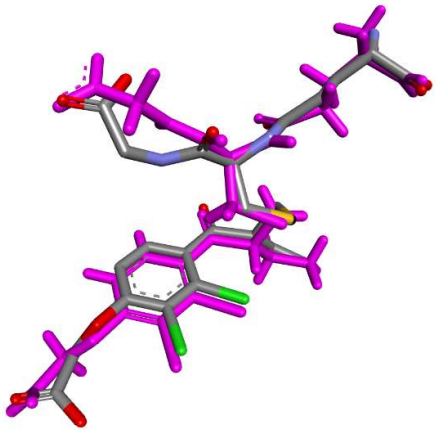

Fig. 2. The real (grey-colored) and predicted positions of the glutathione-etacrynic acid complex inside GST (PDB 11GS) are shown, with an RMSD of 1.8402 Å

The binding site for docking was defined as the amino acid residues surrounding the binding region of GST. To ensure comprehensive coverage of potential interactions, the radius of the docking site was expanded from the default 6.5 Å to 8.5 Å. The glutathione-ethacrynic acid conjugate from the available X-ray crystal structure was used to validate the docking parameters and to benchmark docking scores against those of the predicted complexes. Visualization and analysis of the docking results were performed using BIOVIA Discovery Studio and the built-in PoseView module from LeadIT.

4. Results

4. 1. Chemistry

The target CAAs and DCAAs 2a,b; 3a-h; 4a-d were synthesized using early developed protocols [32, 42], which are based on acylation of corresponding thiazole-bearing amines by chloroacetyl or dichloroacetyl chlorides in the dry dioxane medium with presence of triethylamine. Compounds 2a,b; 3a-h; and 4a-d were obtained with satisfactory yields (58–81 %) and purity. Performed synthetic transformations and structures of synthesized molecules are depicted in Fig. 3.

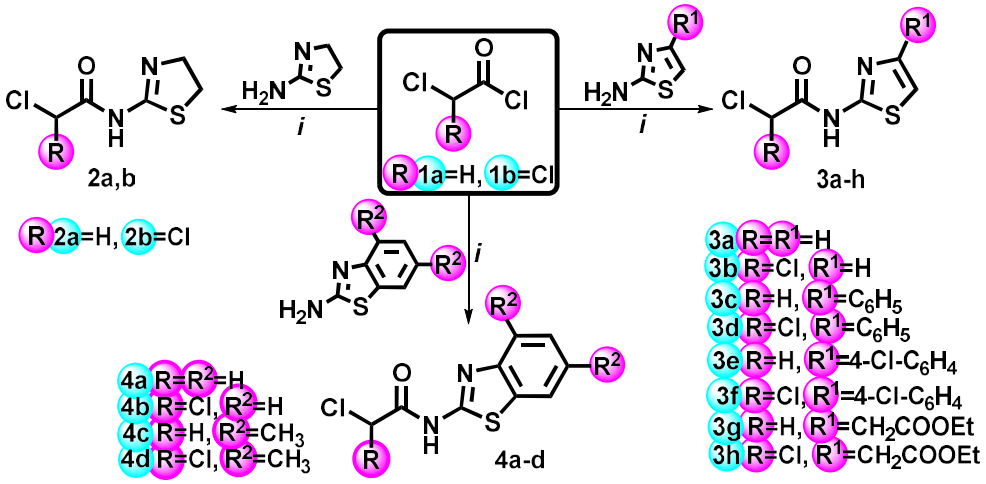

Fig. 3. Synthesis of target chloro- and dichloroacetamides 2a,b; 3a-h; 4a-d. Reagents and conditions: i – corresponding amine (10 mmole), chloroacetyl chloride or dichloroacetyl chloride (10 mmole), triethylamine (10 mmole), dioxane (10ml), stirring 15 minutes (r. t.), and then was heated to 70–80 °C for 30 minutes

The structure of synthesized derivatives 2a,b; 3a-h; 4a-d was confirmed using ^{1}H, ^{13}C NMR, and LC-MS spectra (copies of spectra are presented in the Supplementary Materials). In the ^{1}H NMR spectra of CAAs 3c, 3e, 3g, 4a and DCAAs 3b, 3d, 3f, 3h, 4b signals of aliphatic CH_2 and CH protons appear as singlets at 4.35–4.46 ppm, 6.64–6.71 ppm, correspondingly. The molecular ion peaks observed at the m/z values in the positive ionization mode in the mass spectra confirmed the formation of the target derivatives.

4. 2. Screening of cytotoxic activity on cancer and pseudo-normal cell lines

With the aim to investigate the cytotoxicity of the synthesized compounds 2a,b; 3a-h; 4a-d on various types of cancer and normal cells, MTT assay was applied on myeloproliferative neoplasms cell models (Ba/F3 wt Mouse Pro B-cell line, Ba/F3 CALRins 5 Mouse Pro B-cell line and Ba/F3 CALRdel 52 Mouse Pro B-cell line), human colorectal cancer cells (HT-29), human colon carcinoma cells (HCT-116), human chronic myelogenous Leukemia cells (K562), human acute T cell Leukemia cells (Jurkat), human triple negative breast cancer cells (MDA-MB-231), mice fibroblasts (BALB-3T3), and human epidermal keratinocytes (HaCat) for 72 hours. The IC50 (μM) values for testing compounds were determined using point-to-point analysis and presented in Table 1.

Cytotoxicity screening results revealed that synthesized CAAs possessed significantly higher activity levels towards tested cancer cell lines compared to their dichlorosubstituted analogs (Table 1, Fig. 4 and Supporting Information: Figure S39). The most potent CAAs 3a, 3c, 4c, and 3g demonstrated strong cytotoxic effect with IC50 values ranging from 5.99 up to ≥50 μM toward tested cancer models.

Table 1

The IC50 values of compounds 2a,b; 3a-h; 4a-d on cancer and pseudo-normal cell lines based on MTT test data for 72 h (μM).

Cell lines/ compound	Myeloproliferative neoplasms cell models			Cancer cell lines					Pseudo-normal cell lines	
	Ba/F3 wt	Ba/F3 CALR Ins5	Ba/F3 CALR Del52	HT-29	HCT-116	K562	Jur-kat	MDA-MB-231	BALB-3T3	HaCat
2a	34.77	33.89	≥50	≥50	≥50	48.85	n/d	39.58	≥50	n/d
2b	≥50	≥50	≥50	≥50	≥50	≥50	>50	≥50	≥50	n/d
3a	7.72	7.45	7.88	n/d	34.42	33.12	≥50	7.97	>50	≥50
3b	≥50	≥50	≥50	≥50	≥50	≥50	n/d	≥50	≥50	n/d
3c	6.05	6.78	6.99	27.61	7.92	5.99	6.4	7.67	32.24	≥50
3d	≥50	≥50	≥50	≥50	≥50	≥50	n/d	≥50	≥50	n/d
3e	27.08	8.67	31.41	14.78	49.35	31.34	n/d	14.72	33.61	≥50
3f	≥50	47.05	≥50	≥50	38.60	42.54	n/d	47.54	≥50	≥50
3g	7.34	7.26	9.73	n/d	34.70	36.47	8.54	8.96	n/d	n/d
3h	≥50	≥50	≥50	n/d	≥50	>50	>50	>50	n/d	n/d
4a	25.06	6.42	14.08	33.66	30.62	27.71	n/d	8.60	35.65	n/d
4b	≥50	≥50	≥50	≥50	≥50	≥50	>50	≥50	≥50	n/d
4c	7.08	6.98	7.42	30.33	33.81	19.22	n/d	7.60	4.51	≥50
4d	≥50	≥50	41.90	≥50	≥50	≥50	n/d	47.54	≥50	≥50

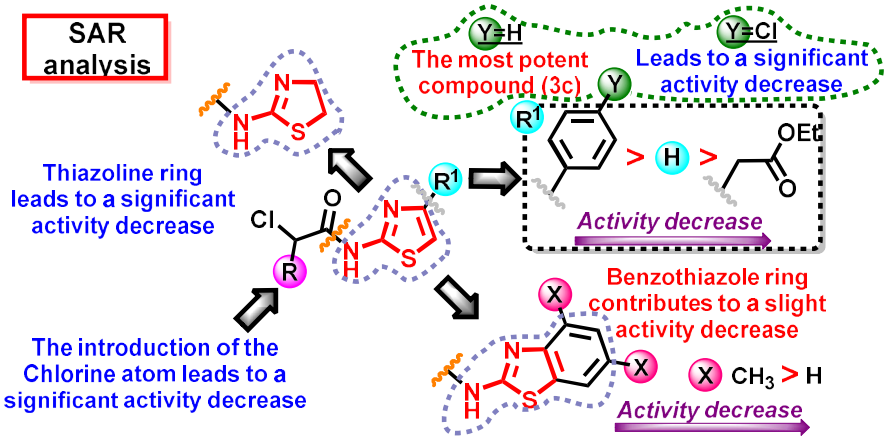

Fig. 4. Some preliminary structure – anticancer activity relationships for the synthesized CAAs and DCAAs 2a,b; 3a-h; 4a-d

4. 3. In silico evaluation of ADMET properties using ADMETlab 3.0

Predictions of some ADMET properties of the studied compounds 3a, 3c, 3g and 4c were performed using ADMETlab 3.0 [43]. The calculated prognostic ADMET parameters are summarized and presented in Supporting Information (Tables 1–3), with key findings highlighted below.

All four compounds comply with major medicinal chemistry rules, including Lipinski's rule of five, which predicts good oral bioavailability based on molecular weight, lipophilicity (log P), hydrogen bond donors (HBD), and acceptors (HBA). They also meet the GSK rule, which is designed to minimize toxicity risks in drug development. However, compounds 3c and 4c violated Pfizer's rule, which flags potential toxicity due to high log P and molecular weight. Compound 3g exhibited the most balanced properties, with acceptable molecular weight, polar surface area (TPSA), log P, and an appropriate Fsp^3 score, indicating potential for good solubility and absorption.

Predicted absorption data indicated low permeability for all compounds through MDCK and Caco-2 models. All compounds are unlikely substrates or inhibitors of P-glycoprotein, ensuring favorable pharmacokinetics. Human intestinal absorption (HIA) predictions suggested poor absorption for all derivatives, particularly 4c and 3c. Plasma protein binding (PPB) was high for compounds 3c and 4c, indicating a low free-drug fraction, while 3g showed moderate binding, which may result in a better therapeutic index. However, none of the compounds are predicted to efficiently cross the blood-brain barrier (BBB), reducing the likelihood of central nervous system (CNS) side effects.

All compounds exhibited low plasma clearance, with 3g showing moderate clearance. The predicted half-life was short for all derivatives except 3a, which showed an intermediate half-life, indicating the need for less frequent dosing. Regarding toxicity, compounds 3c and 4c had higher probabilities of human hepatotoxicity (H-HT) and mutagenicity (AMES). In contrast, 3g displayed the lowest risks of hepatotoxicity and mutagenicity, making it the safest candidate.

Compounds 3c and 4c demonstrated strong potential for being PPARγ agonists, while 3g showed modest activity, suggesting potential metabolic or anti-inflammatory applications. Notably, 3g also displayed low probabilities of being an estrogen receptor (ER) agonist or aromatase inhibitor, reducing concerns about off-target hormonal effects.

The predicted ADMET profiles suggest that compound 3g has the most favorable balance of drug-like properties, including reduced toxicity risks, moderate clearance, and metabolic stability. This makes it the most promising candidate for further pharmacological evaluation.

4. 4. Quantum chemical calculations

The anticancer activity screening result showed a significant difference between synthesized CAAs and their dichlorosubstituted analogs. Since CAAs possess higher activity than DCAAs and differ only with the presence in the structure of one additional Chlorine atom, their action could be expected to mainly depend on the reactivity of the carbon atom bound to one or two chlorine atoms. To explain the difference in anticancer activity in structure-related compounds, quantum-chemical calculations of their electronic features were carried out for some synthesized CAAs and DCAAs.

The molecules' electrophilic properties depend on their energy levels' location. The energy levels' relative arrangement and the shape of molecular orbitals of some CAAs and DCAAs are presented in Fig. 5. As presented, two chlorine atoms create a greater acceptor effect, and the energy levels shift down. The LUMO energy is more affected. In addition, in DCAAs, the LUMO is more concentrated on the same side of the molecule as the terminal carbon with two chlorine atoms. All this indicates greater electrophilic properties of DCAAs compared to CAAs. However, it is known that the results of quantum-chemical calculations of the CAAs reactivity showed no correlation

with the warhead-associated electrophilicity index [44]. Therefore, their alkylating ability will be determined more by the reaction mechanism than by electronic effects in the molecule.

CAAs and DCAAs covalent binding occurs due to the halogen substitution on a cysteine residue. In this case, the reaction takes place either through the carbocation formation (by the S_N1 mechanism) or through a transition state (by the S_N2 mechanism), in both cases the carbon atom changes its initial sp^3-hybridization to sp^2-hybridization with an approximately perpendicular *p*-orbital. This *p*-orbital enters into conjugation with the other conjugated system, and in the case of DCAAs, another chlorine atom is also included in this system, which in this case will already exhibit the M+ effect and reduce the electron density on the carbocation, which will reduce its reactivity. Two such cations were calculated, which are formed when a chlorine atom is removed from CAAs 4a (cation A) and from DCAAs (cation B), the energy and shape of the frontier orbitals are shown in Fig. 6. The donor effect of the chlorine atom in the transition state affects the location of the energy levels, which are higher in the B cation containing the conjugated chlorine atom. The Fukui indices were calculated for the carbon atom of carbocation A $f^+(C^+)$=0.191 and B $f^+(C^+)$=0.162, which indicating a greater ability of the intermediate carbocation A to be attacked by a nucleophile.

[45] also noted the lower reactivity of DCAAs compared to CAAs. In the same article, they show the substitution products' instability in an aqueous medium, where the DCAAs-thiol adduct easily hydrolyzes in an aqueous solution. In contrast, the CAAs-thiol adduct does not hydrolyze. In addition, due to the DCAAs-thiol adduct hydrolysis, the product does not contain chlorine atoms and will not be able to further act as an alkylating agent.

4. 5. Molecular docking

According to the reports, biologically active CAAs (including herbicides) can interact with glutathione [46–49]. This interaction is suggested to contribute to their primary mode of action as well as associated with toxic side effects. However, some compounds, such as etacrynic acid, which can covalently bind to glutathione, have been shown to act as ligands that block GST activity [50–52]. Such GST inhibition may enhance the efficacy of chemotherapy regimens by increasing the levels of reactive oxygen species (ROS), thereby promoting cellular damage [53, 54]. If these conjugates exhibit strong affinity for GST, they could also function as GST inhibitors. This approach may be useful for anticancer therapy or as an adjunct to existing treatments to reduce resistance or enhance the efficacy of the selected chemotherapy regimen [50, 55–58].

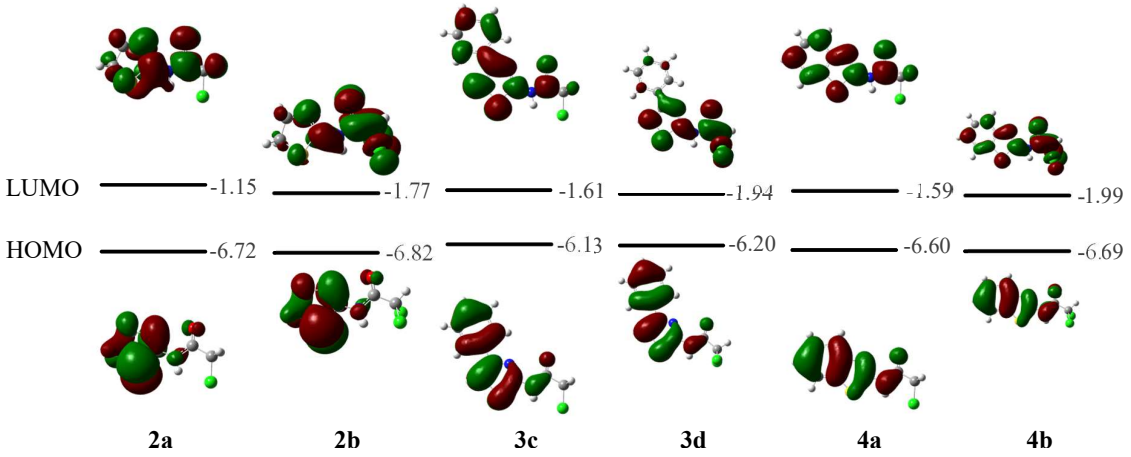

Fig. 5. Energy and shape of frontier molecular orbitals of some synthesized derivatives of CAAs and DCAAs

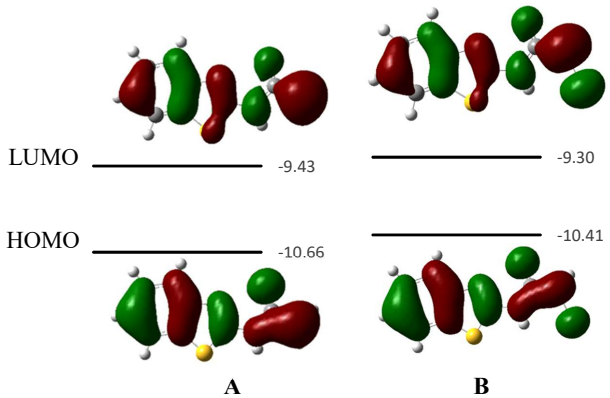

Fig. 6. The energy and shape of the frontier molecular orbitals of the intermediate cations formed during the chlorine anion removed from 4a (A) and 4b (B)

Therefore, we aimed to evaluate the affinity of potential glutathione-CAAs conjugates as GST inhibitors. The obtained FlexX docking scores are presented in Table 2.

Table 2

The FlexX docking scores of the predicted glutathione-CAAs conjugates and complex with the etacrynic acid

Compounds	GST, (PDB 11GS) FlexX docking score
2a	–26.5358
3a	–28.9050
3c	–34.4758
3e	–33.0665
3g	–29.8119
4a	–33.2909
4c	–31.4291
GSH-EAA complex	–29.2766

Most conjugates demonstrate improved binding affinity compared to the native glutathione-etacrynic acid complex. The best docking score was obtained for the glutathione-3c complex. As shown in Fig. 7, the 4-phenylthiazol-2-yl motif fits well into the hydrophobic pocket formed by several lipophilic amino acids, including Ile104, Tyr108, Val10, Tyr7, and Phe8. Other CAAs interact in a similar manner; however, in the case of compound 3c, the presence of a phenyl substituent increases the number of amino acids involved in lipophilic interactions.

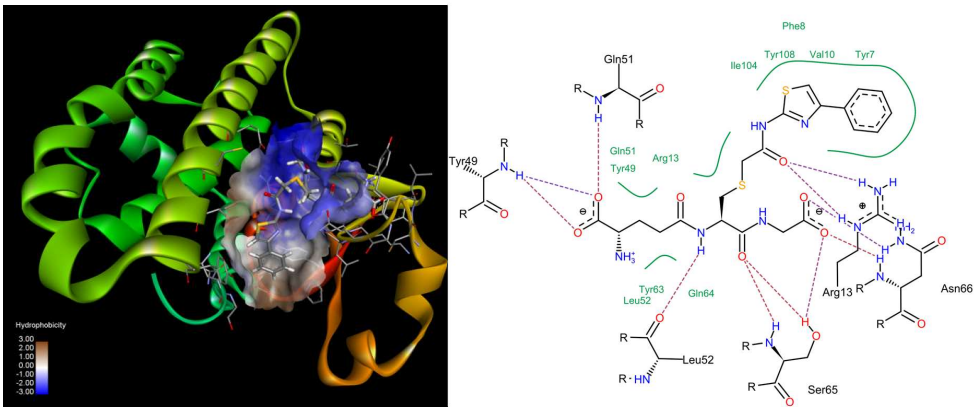

Fig. 7. The 3D and 2D interaction diagrams of the glutathione-3c conjugate with GST (PDB code 11GS). Pink indicates hydrogen bonds, while green represents lipophilic interactions

5. Discussion

It has been established that the synthesized 2-chloroacetamides exhibit superior cytotoxicity compared to the dichlorosubstituted analogs. While dichlorosubstituted analogs 3d, 3b, 4d, and 3h decreased cell viability to a lesser extent with IC50 in the range of 41.90 up to ≥50 μM. Compounds 3e, 2a, and 4a demonstrated moderate cytotoxic effect, with IC50 values predominantly within 30–40 μM range. In contrast, DCAAs 3f, 2b, and 4b did not affect the viability of both cancer and pseudo-normal cell lines (MDA-MB-231, K562, HT-29, HCT-116, Jurkat, and Ba/F3wt, BALB-3T3, HaCat respectively). It was also observed that thiazoline-bearing derivative 2a exhibited lower cytotoxicity across all cell lines compared to thiazole and benzothiazole analogs 3a, 4c and 4a. Notably, while DCAAs are nearly inactive, the highest sensitivity to CAAs was observed in myeloproliferative disease model cells carrying calreticulin gene mutations (Ba/F3CALRins5 and Ba/F3CALRdel52), their wild-type counterpart Ba/F3wt cells, human acute T cell leukemia (Jurkat cell line) and the triple-negative breast cancer cells MDA-MB-231. Lower sensitivity was demonstrated by colon cancer cell lines HT-29, HCT-116, and the chronic myeloid leukemia cell line K562. Furthermore, CAAs reduced BALB-3T3 fibroblast viability to some extent.

Summarizing the obtained results of quantum chemical studies, we can see that the lower activity of DCAAs compared to CAAs is due to a combination of electronic effects and the intermediates' stability. The DCAAs' higher electrophilic properties, due to the chlorine atoms acceptor effect that lowers the LUMO, can reduce the carbocations reactivity, especially in the S_N1 mechanism, where the chlorine donor effect reduces the electron density. In the S_N2 mechanism, conjugation with chlorine atoms probably complicates the formation of a stable transition state. In addition, the lower reactivity observed in DCAAs may also be due to steric hindrance and DCAAs-thiol adduct instability in an aqueous environment, which leads to its hydrolysis and alkylating properties loss. CAAs-thiol adducts, on the other hand, show higher stability, which may explain their higher activity. Thus, the differences in activity are likely due to the chemical properties of the intermediates and the stability of the products formed. This requires further research to determine the applications of DCAAs.

Furthermore, the FlexX docking scores of the conjugates during *in silico* simulation corroborate the cytotoxicity data: the improved binding affinities of glutathione-CAA conjugates, especially the glutathione-3c complex, support the hypothesis that GST inhibition may be a key action mechanism. Nevertheless, one disadvantage is that CAAs may also interact with other thiol-containing enzymes, which could contribute to complex cytotoxic effects. When compared with other studies – for example, those reporting on similar anticancer scaffolds and their GST interactions [50, 51, 53–56] – our results agree regarding the importance of electronic properties and binding stability. However, discrepancies in IC50 values among different cell lines indicate that additional factors, such as cell-specific uptake and metabolism, may also play significant roles.

In summary, the advantages of our study include the integrated approach combining *in vitro* cytotoxicity,

quantum chemical analysis, and molecular docking, which provides a comprehensive understanding of the «structure-activity» relationships in these compounds.

Practical relevance. The results of this study provide a valuable foundation for the rational design of novel anticancer agents. By elucidating the «structure-activity» relationships of 2-chloroacetamides and 2,2-dichloroacetamides through integrated *in vitro* cytotoxicity assays, quantum chemical calculations, ADMET profiling, and molecular docking studies, our findings can guide the molecular scaffolds optimization to achieve improved efficacy and selectivity. In particular, the demonstrated potential of CAAs to interact with glutathione and inhibit GST activity offers a promising strategy for targeted anticancer therapy. Furthermore, the comprehensive computational approach employed here can serve as a predictive platform for future drug development, facilitating the early identification of candidates with favorable pharmacokinetic and toxicity profiles.

Research limitations. Despite the promising outcomes, several limitations must be acknowledged. The cytotoxicity and ADMET evaluations were performed exclusively *in vitro* and through *in silico* models, which may not fully replicate *in vivo* biological conditions. The variability among cell lines and the inherent limitations of current computational methods – such as the approximations used in quantum chemical calculations and docking simulations – may affect the precision of the predicted reactivity and binding interactions. Moreover, potential off-target effects and these compounds' complex metabolism in a living system remain to be elucidated, thus restricting the immediate clinical applicability of the findings.

Prospects for further research. The present study opens numerous avenues for future investigations. Further research should include *in vivo* studies to validate the anticancer efficacy and safety of the most promising CAAs, particularly those exhibiting favorable ADMET profiles. Detailed mechanistic studies are warranted to fully elucidate the role of GST inhibition and other molecular interactions in mediating cytotoxic effects. Advancements in computational modeling – such as incorporating active learning into docking protocols – could further refine the prediction of molecular reactivity and binding affinity. Additionally, exploring combination therapies and alternative drug delivery systems may enhance these compounds' therapeutic potential, ultimately contributing to developing innovative, targeted anticancer drugs.

6. Conclusion

In the present paper, the synthesis of a series of 2-chloro- and 2,2-dichloroacetamides bearing thiazole scaffolds as potential anticancer agents is reported. Anticancer and cytotoxicity properties of all the compounds have been evaluated in the panels of cancer and pseudo-normal cell lines. Synthesized 2-chloroacetamides possessed high and moderate activity levels towards calreticulin gene mutations (Ba/F3CALRins5 and Ba/F3CALRdel52), their wild-type counterpart Ba/F3wt cells, human acute T cell leukemia (Jurkat cell line) and the triple-negative breast cancer cells MDA-MB-231. Meanwhile, synthesized 2,2-dichloroacetamide analogs were found to be almost inactive in the tested lines. Performed quantum chemical calculations suggest that the differences in activity are likely due to the chemical properties of the intermediates and the stability of the products formed. The docking studies results demonstrate that most glutathione-2-chloroacetamides conjugates exhibit higher binding affinity to GST compared to the native glutathione-etacrynic acid complex. These findings suggest that the cytotoxic effects of the tested 2-chloroacetamides may be linked to their interaction with glutathione and subsequent inhibition of GST activity.

Conflict of interest

The authors declare that they have no conflict of interest concerning this study, including financial, personal, authorship, or any other, that could affect the study and its results presented in this article.

Funding

This research was funded by the National Research Foundation of Ukraine Grant No. 2023.05/0021 and Grant No. 2023.03/0104

Data availability

The data presented in this study are available in this article.

Use of artificial intelligence

The authors confirm that they did not use artificial intelligence technologies when creating the current work.

Acknowledgments

The authors are sincerely grateful to Prof. Robert Kralovics for the cell lines provided for research. The authors thank all the brave defenders of Ukraine who made the performance of this study possible.

References

1. Bedard, P. L., Hyman, D. M., Davids, M. S., Siu, L. L. (2020). Small molecules, big impact: 20 years of targeted therapy in oncology. The Lancet, 395 (10229), 1078–1088. https://doi.org/10.1016/s0140-6736(20)30164-1

2. Zhong, L., Li, Y., Xiong, L., Wang, W., Wu, M., Yuan, T. et al. (2021). Small molecules in targeted cancer therapy: advances, challenges, and future perspectives. Signal Transduction and Targeted Therapy, 6 (1). https://doi.org/10.1038/s41392-021-00572-w

3. Olgen, S. (2018). Overview on Anticancer Drug Design and Development. Current Medicinal Chemistry, 25 (15), 1704–1719. https://doi.org/10.2174/0929867325666171129215610

4. Steinbrueck, A., Sedgwick, A. C., Brewster, J. T., Yan, K.-C., Shang, Y., Knoll, D. M. et al. (2020). Transition metal chelators, pro-chelators, and ionophores as small molecule cancer chemotherapeutic agents. Chemical Society Reviews, 49(12), 3726–3747. https://doi.org/10.1039/c9cs00373h

5. Zhang, J., Duan, D., Song, Z., Liu, T., Hou, Y., Fang, J. (2020). Small molecules regulating reactive oxygen species homeostasis for cancer therapy. Medicinal Research Reviews, 41 (1), 342–394. https://doi.org/10.1002/med.21734

6. Hassan, G. S., El-Messery, S. M., Al-Omary, F. A. M., El-Subbagh, H. I. (2012). Substituted thiazoles VII. Synthesis and antitumor activity of certain 2-(substituted amino)-4-phenyl-1,3-thiazole analogs. Bioorganic & Medicinal Chemistry Letters, 22 (20), 6318–6323. https://doi.org/10.1016/j.bmcl.2012.08.095

7. Padhariya, K. N., Athavale, M., Srivastava, S., Kharkar, P. S. (2019). Substituted chloroacetamides as potential cancer stem cell inhibitors: Synthesis and biological evaluation. Drug Development Research, 81 (3), 356–365. https://doi.org/10.1002/ddr.21628

8. Demirci, S., Uslu, H., Mermer, A., Yesilay, G., Betul Aydin, Z. (2024). Synthesis and Characterization of Propofol-Like Compounds, Anticancer Activities and Investigation of Their Anesthetic Effects by Molecular Docking. ChemistrySelect, 9 (17). https://doi.org/10.1002/slct.202400431

9. Lesyk, R., Vladzimirska, O., Zimenkovsky, B., Golota, S., Nektgayev, I., Cherpak, O. et al. (2002). Synthesis and antiinflammatory activity of novel 3-(2,3-dimethyl-1-phenyl-4-pyrazolon-5-yl)-4-thiazolidones. Bollettino Chimico Farmaceutico, 141 (3), 197–201.

10. Havryshchuk, L., Horishny, V., Rushchak, N., Lesyk, R. (2024). Dichloroacetic acid derivatives as potential anti-tumor and anti-inflammatory agents. ScienceRise: Pharmaceutical Science, 1 (47), 60–78. https://doi.org/10.15587/2519-4852.2024.299229

11. Fumarola, C., Bozza, N., Castelli, R., Ferlenghi, F., Marseglia, G., Lodola, A. et al. (2019). Expanding the Arsenal of FGFR Inhibitors: A Novel Chloroacetamide Derivative as a New Irreversible Agent With Anti-proliferative Activity Against FGFR1-Amplified Lung Cancer Cell Lines. Frontiers in Oncology, 9. https://doi.org/10.3389/fonc.2019.00179

12. Bogdanović, A., Marinković, A., Stanojković, T., Grozdanić, N., Janakiev, T., Cvijetić, I., Petrović, S. (2025). Synthesis, antimicrobial, anticancer activity, 3D QSAR, ADMET properties, and in silico target fishing of novel N,N-disubstituted chloroacetamides. Journal of Molecular Structure, 1321, 140075. https://doi.org/10.1016/j.molstruc.2024.140075

13. Müller, M. P., Jeganathan, S., Heidrich, A., Campos, J., Goody, R. S. (2017). Nucleotide based covalent inhibitors of KRas can only be efficient in vivo if they bind reversibly with GTP-like affinity. Scientific Reports, 7 (1). https://doi.org/10.1038/s41598-017-03973-6

14. Xiong, Y., Lu, J., Hunter, J., Li, L., Scott, D., Choi, H. G. et al. (2016). Covalent Guanosine Mimetic Inhibitors of G12C KRAS. ACS Medicinal Chemistry Letters, 8 (1), 61–66. https://doi.org/10.1021/acsmedchemlett.6b00373

15. Hossain, M., Roayapalley, P. K., Sakagami, H., Satoh, K., Bandow, K., Das, U., Dimmock, J. R. (2022). Dichloroacetyl Amides of 3,5-Bis(benzylidene)-4-piperidones Displaying Greater Toxicity to Neoplasms than to Non-Malignant Cells. Medicines, 9 (6), 35. https://doi.org/10.3390/medicines9060035

16. Fereidoonnezhad, M., Tabaei, S. M. H., Sakhteman, A., Seradj, H., Faghih, Z., Faghih, Z. et al. (2020). Design, synthesis, molecular docking, biological evaluations and QSAR studies of novel dichloroacetate analogues as anticancer agent. Journal of Molecular Structure, 1221, 128689. https://doi.org/10.1016/j.molstruc.2020.128689

17. Zare, S., Ramezani, Z., Ghadiri, A. A., Fereidoonnezhad, M. (2023). Synthesis of N-(2-(tert-Butylamino)-2-oxoethyl)-2,2-dichloro-N-aryl(alkyl)acetamides as Anticancer Agents: Molecular Modeling and Biological Evaluations. ChemistrySelect, 8 (1). https://doi.org/10.1002/slct.202203931

18. Li, T., Yang, Y., Cheng, C., Tiwari, A. K., Sodani, K., Zhao, Y. et al. (2012). Design, synthesis and biological evaluation of N-arylphenyl-2,2-dichloroacetamide analogues as anti-cancer agents. Bioorganic & Medicinal Chemistry Letters, 22 (23), 7268–7271. https://doi.org/10.1016/j.bmcl.2012.07.057

19. Zhang, S.-L., Zhang, W., Xiao, Q., Yang, Z., Hu, X., Wei, Z., Tam, K. Y. (2016). Development of dichloroacetamide pyrimidines as pyruvate dehydrogenase kinase inhibitors to reduce cancer cell growth: synthesis and biological evaluation. RSC Advances, 6 (82), 78762–78767. https://doi.org/10.1039/c6ra14060b

20. Trapella, C., Voltan, R., Melloni, E., Tisato, V., Celeghini, C., Bianco, S. et al. (2015). Design, Synthesis, and Biological Characterization of Novel Mitochondria Targeted Dichloroacetate-Loaded Compounds with Antileukemic Activity. Journal of Medicinal Chemistry, 59 (1), 147–156. https://doi.org/10.1021/acs.jmedchem.5b01165

21. Zhang, S.-L., Hu, X., Zhang, W., Yao, H., Tam, K. Y. (2015). Development of pyruvate dehydrogenase kinase inhibitors in medicinal chemistry with particular emphasis as anticancer agents. Drug Discovery Today, 20 (9), 1112–1119. https://doi.org/10.1016/j.drudis.2015.03.012

22. Hossain, M., Roth, S., Dimmock, J. R., Das, U. (2022). Cytotoxic derivatives of dichloroacetic acid and some metal complexes. Archiv Der Pharmazie, 355 (11). https://doi.org/10.1002/ardp.202200236

23. Yang, Y., Shang, P., Cheng, C., Wang, D., Yang, P., Zhang, F. et al. (2010). Novel N-phenyl dichloroacetamide derivatives as anticancer reagents: Design, synthesis and biological evaluation. European Journal of Medicinal Chemistry, 45 (9), 4300–4306. https://doi.org/10.1016/j.ejmech.2010.06.032

24. Abdel-Latif, E., Fahad, M. M., El-Demerdash, A., Ismail, M. A. (2020). Synthesis and biological evaluation of some heterocyclic scaffolds based on the multifunctional N-(4-acetylphenyl)-2-chloroacetamide. Journal of Heterocyclic Chemistry, 57 (8), 3071–3081. https://doi.org/10.1002/jhet.4012

25. Zimenkovsky, B., Lesyk, R., Vladzimirska, O., Nektegayev, I., Golota, S., Chorniy, I. (1999). The structure – anti-inflammatory activity relationship among thiazolidones: Conclusion from scientific programme. Journal of Pharmacy and Pharmacology, 51, 264.

26. Abdel-Latif, E., Fahad, M. M., Ismail, M. A. (2019). Synthesis ofN-aryl 2-chloroacetamides and their chemical reactivity towards various types of nucleophiles. Synthetic Communications, 50 (3), 289–314. https://doi.org/10.1080/00397911.2019.1692225

27. Huang, F., Han, X., Xiao, X., Zhou, J. (2022). Covalent Warheads Targeting Cysteine Residue: The Promising Approach in Drug Development. Molecules, 27 (22), 7728. https://doi.org/10.3390/molecules27227728

28. Bonnet, S., Archer, S. L., Allalunis-Turner, J., Haromy, A., Beaulieu, C., Thompson, R. et al. (2007). A Mitochondria-K+ Channel Axis Is Suppressed in Cancer and Its Normalization Promotes Apoptosis and Inhibits Cancer Growth. Cancer Cell, 11 (1), 37–51. https://doi.org/10.1016/j.ccr.2006.10.020

29. Koltai, T., Fliegel, L. (2024). Dichloroacetate for Cancer Treatment: Some Facts and Many Doubts. Pharmaceuticals, 17 (6), 744. https://doi.org/10.3390/ph17060744

30. Alizadeh, S. R., Hashemi, S. M. (2021). Development and therapeutic potential of 2-aminothiazole derivatives in anticancer drug discovery. Medicinal Chemistry Research, 30 (4), 771–806. https://doi.org/10.1007/s00044-020-02686-2

31. Wan, Y., Long, J., Gao, H., Tang, Z. (2021). 2-Aminothiazole: A privileged scaffold for the discovery of anti-cancer agents. European Journal of Medicinal Chemistry, 210, 112953. https://doi.org/10.1016/j.ejmech.2020.112953

32. Mishchenko, M., Shtrygol', S., Lozynskyi, A., Khomyak, S., Novikov, V., Karpenko, O. et al. (2021). Evaluation of Anticonvulsant Activity of Dual COX-2/5-LOX Inhibitor Darbufelon and Its Novel Analogues. Scientia Pharmaceutica, 89 (2), 22. https://doi.org/10.3390/scipharm89020022

33. Geronikaki, A., Theophilidis, G. (1992). Synthesis of 2-(aminoacetylamino)thiazole derivatives and comparison of their local anaesthetic activity by the method of action potential. European Journal of Medicinal Chemistry, 27 (7), 709–716. https://doi.org/10.1016/0223-5234(92)90091-e

34. Ivasechko, I., Yushyn, I., Roszczenko, P., Senkiv, J., Finiuk, N., Lesyk, D. et al. (2022). Development of Novel Pyridine-Thiazole Hybrid Molecules as Potential Anticancer Agents. Molecules, 27 (19), 6219. https://doi.org/10.3390/molecules27196219

35. Frisch, M., Trucks, G., Schlegel, H., Scuseria, G., Robb, M., Cheeseman, J. et al. (2016). Gaussian 09, Revision A.02. Wallingford: Gaussian Inc.

36. Dennington, R., Keith, T., Millam, J. (2016). GaussView 5.0.8. Shawnee Mission: Semichem Inc.

37. Halgren, T. A. (1996). Merck molecular force field. I. Basis, form, scope, parameterization, and performance of MMFF94. Journal of Computational Chemistry, 17 (5-6), 490–519. https://doi.org/10.1002/(sici)1096-987x(199604)17:5/6<490::aid-jcc1>3.0.co;2-p

38. Hanwell, M. D., Curtis, D. E., Lonie, D. C., Vandermeersch, T., Zurek, E., Hutchison, G. R. (2012). Avogadro: an advanced semantic chemical editor, visualization, and analysis platform. Journal of Cheminformatics, 4 (1). https://doi.org/10.1186/1758-2946-4-17

39. Oakley, A. J., Lo Bello, M., Mazzetti, A. P., Federici, G., Parker, M. W. (1997). The glutathione conjugate of ethacrynic acid can bind to human pi class glutathione transferase P1-1 in two different modes. FEBS Letters, 419 (1), 32–36. https://doi.org/10.1016/s0014-5793(97)01424-5

40. Kramer, B., Rarey, M., Lengauer, T. (1999). Evaluation of the FLEXX incremental construction algorithm for protein-ligand docking. Proteins: Structure, Function, and Genetics, 37 (2), 228–241. https://doi.org/10.1002/(sici)1097-0134(19991101)37:2<228::aid-prot8>3.0.co;2-8

41. Yusuf, D., Davis, A. M., Kleywegt, G. J., Schmitt, S. (2008). An Alternative Method for the Evaluation of Docking Performance: RSR vs RMSD. Journal of Chemical Information and Modeling, 48 (7), 1411–1422. https://doi.org/10.1021/ci800084x

42. Yushyn, I., Holota, S., Lesyk, R. (2022). 2,2-Dichloro-N-[5-[2-[3-(4-methoxyphenyl)-5-phenyl-3,4-dihydro-2H-pyrazol-2-yl]-2-oxoethyl]sulfanyl-1,3,4-thiadiazol-2-yl]acetamide. Molbank, 2022(1), M1328. https://doi.org/10.3390/m1328

43. ADMETlab 3.0. Scbdd.com. Available at: https://admetlab3.scbdd.com/server/evaluation

44. Ree, N., Göller, A. H., Jensen, J. H. (2024). Automated quantum chemistry for estimating nucleophilicity and electrophilicity with applications to retrosynthesis and covalent inhibitors. Digital Discovery, 3 (2), 347–354. https://doi.org/10.1039/d3dd00224a

45. Yamane, D., Tetsukawa, R., Zenmyo, N., Tabata, K., Yoshida, Y., Matsunaga, N. et al. (2023). Expanding the Chemistry of Dihaloacetamides as Tunable Electrophiles for Reversible Covalent Targeting of Cysteines. Journal of Medicinal Chemistry, 66 (13), 9130–9146. https://doi.org/10.1021/acs.jmedchem.3c00737

46. Coleman, S., Linderman, R., Hodgson, E., Rose, R. L. (2000). Comparative metabolism of chloroacetamide herbicides and selected metabolites in human and rat liver microsomes. Environmental Health Perspectives, 108 (12), 1151–1157. https://doi.org/10.1289/ehp.001081151

47. Bernasinska, J., Duchnowicz, P., Koter-Michalak, M., Koceva-Chyla, A. (2013). Effect of safeners on damage of human erythrocytes treated with chloroacetamide herbicides. Environmental Toxicology and Pharmacology, 36 (2), 368–377. https://doi.org/10.1016/j.etap.2013.04.010

48. Jablonkai, I., Dutka, F. (1992). Preparative-scale synthesis and physicochemical properties of cysteine and glutathione conjugates of chloroacetamides. Journal of Agricultural and Food Chemistry, 40 (3), 506–508. https://doi.org/10.1021/jf00015a029

49. Ma, X., Zhang, Y., Guan, M., Zhang, W., Tian, H., Jiang, C. et al. (2021). Genotoxicity of chloroacetamide herbicides and their metabolites in vitro and in vivo. International Journal of Molecular Medicine, 47 (6). https://doi.org/10.3892/ijmm.2021.4936

50. Ploemen, J. H. T. M., Ommen, B. V., Bogaards, J. J. P., Van Bladeren, P. J. (1993). Ethacrynic acid and its glutathione conjugate as inhibitors of glutathioneS-transferases. Xenobiotica, 23 (8), 913–923. https://doi.org/10.3109/00498259309059418

51. Burgess, E. R., Mishra, S., Yan, X., Guo, Z., Geden, C. J., Miller, J. S., Scharf, M. E. (2024). Differential interactions of ethacrynic acid and diethyl maleate with glutathione S-transferases and their glutathione co-factor in the house fly. Pesticide Biochemistry and Physiology, 205, 106170. https://doi.org/10.1016/j.pestbp.2024.106170

52. Emre Erat, Y., Rümeysa Erat, A., Erat, M. (2023). Inhibitory Effect of Ascorbic Acid on Glutathione S-transferase from Human Erythrocytes. Current Enzyme Inhibition, 19 (3), 188–194. https://doi.org/10.2174/1573408019666230530095315

53. Hellou, J., Ross, N. W., Moon, T. W. (2012). Glutathione, glutathione S-transferase, and glutathione conjugates, complementary markers of oxidative stress in aquatic biota. Environmental Science and Pollution Research, 19 (6), 2007–2023. https://doi.org/10.1007/s11356-012-0909-x

54. Tew, K. D. (2016). Glutathione-Associated Enzymes In Anticancer Drug Resistance. Cancer Research, 76 (1), 7–9. https://doi.org/10.1158/0008-5472.can-15-3143

55. Mahajan, S., Atkins, W. M. (2005). The chemistry and biology of inhibitors and pro-drugs targeted to glutathione S-transferases. Cellular and Molecular Life Sciences, 62 (11), 1221–1233. https://doi.org/10.1007/s00018-005-4524-6

56. Townsend, D. M., Tew, K. D. (2003). The role of glutathione-S-transferase in anti-cancer drug resistance. Oncogene, 22 (47), 7369–7375. https://doi.org/10.1038/sj.onc.1206940

57. Gülçin, İ., Scozzafava, A., Supuran, C. T., Akıncıoğlu, H., Koksal, Z., Turkan, F., Alwasel, S. (2015). The effect of caffeic acid phenethyl ester (CAPE) on metabolic enzymes including acetylcholinesterase, butyrylcholinesterase, glutathione S-transferase, lactoperoxidase, and carbonic anhydrase isoenzymes I, II, IX, and XII. Journal of Enzyme Inhibition and Medicinal Chemistry, 31 (6), 1095–1101. https://doi.org/10.3109/14756366.2015.1094470

58. Ozgencli, I., Kilic, D., Guller, U., Ciftci, M., Kufrevioglu, O. I., Budak, H. (2019). A Comparison of the Inhibitory Effects of Anti-Cancer Drugs on Thioredoxin Reductase and Glutathione S-Transferase in Rat Liver. Anti-Cancer Agents in Medicinal Chemistry, 18 (14), 2053–2061. https://doi.org/10.2174/1871520618666180910093335

Received 05.11.2024
Received in revised form 24.12.2024
Accepted 04.02.2025
Published 28.02.2025

Liubomyr Havryshchuk, Assistant Professor, Department of Chemistry, Pharmaceutical Analysis and Postgraduate Education, Ivano-Frankivsk National Medical University
Halytska str., 2, Ivano-Frankivsk, Ukraine, 76018

Volodymyr Horishny, PhD, Associate Professor, Department of Pharmaceutical, Organic and Bioorganic Chemistry, Danylo Halytsky Lviv National Medical University, Pekarska str., 69, Lviv, Ukraine, 79010

Iryna Ivasechko, PhD, Junior Researcher, Department of Regulation of Cell Proliferation and Apoptosis, Institute of Cell Biology, Drahomanova str., 14/16, Lviv, Ukraine, 79005

Yuliia Kozak, PhD, Junior Researcher, Department of Regulation of Cell Proliferation and Apoptosis, Institute of Cell Biology, Drahomanova str., 14/16, Lviv, Ukraine, 79005

Dmytro Melnyk, PhD, Associate Professor, Department of Chemistry, Pharmaceutical Analysis and Postgraduate Education, Ivano-Frankivsk National Medical University, Halytska str., 2, Ivano-Frankivsk, Ukraine, 76018

Dmytro Khylyuk, Assistant Professor, Department of Organic Chemistry, Medical University of Lublin, Aleje Racławickie, 1, Lublin, Poland, 20-059

Myroslava Kusiy, PhD, Associate Professor, Head of Department, Department of Applied Mathematics and Mechanics, Lviv State University of Life Safety, Kleparivska str., 79, Lviv, Ukraine, 79010

Victoria Serhiyenko, Doctor of Medical Sciences, Professor, Vice-Rector for Research, Danylo Halytsky Lviv National Medical University, Pekarska str., 69, Lviv, Ukraine, 79010

Nataliya Finiuk, PhD, Researcher, Department of Regulation of Cell Proliferation and Apoptosis, Institute of Cell Biology, Drahomanova str., 14/16, Lviv, Ukraine, 79005

Rostyslav Stoika, Doctor of Biological Sciences, Professor, Corresponding Member of the National Academy of Sciences of Ukraine, Department of Regulation of Cell Proliferation and Apoptosis, Institute of Cell Biology, Drahomanova str., 14/16, Lviv, Ukraine, 79005

Serhii Holota, PhD, Associate Professor, Department of Pharmaceutical, Organic and Bioorganic Chemistry, Danylo Halytsky Lviv National Medical University, Pekarska str., 69, Lviv, Ukraine, 79010

Roman Lesyk*, University of Information Technology and Management in Rzeszow, Sucharskiego str., 2, Rzeszow, Poland, 35-225, Doctor of Pharmaceutical Sciences, Professor, Head of Department, Department of Pharmaceutical, Organic and Bioorganic Chemistry, Danylo Halytsky Lviv National Medical University, Pekarska str., 69, Lviv, Ukraine, 79010

***Corresponding author:** Roman Lesyk, e-mail: dr_r_lesyk@org.lviv.net, roman.lesyk@gmail.com*